Ann. Geophys. Discuss., https://doi.org/10.5194/angeo-2018-122
Manuscript under review for journal Ann. Geophys.
Discussion started: 8 November 2018

Geomagnetic Conjugate Observations of Ionospheric Disturbances in response to North Korea Underground Nuclear Explosion on 3 September 2017

Yi Liu, Chen Zhou*, Qiong Tang, Guanyi Chen, and Zhengyu Zhao

Department of Space Physics, School of Electronic Information, Wuhan University, Wuhan, China

Corresponding to: chenzhou@whu.edu.cn

Key points:

1. Geomagnetic conjugate ionospheric disturbances related to UNE were observed by IGS stations and Swarm satellite.
2. Radial propagation velocity from the UNE epicenter was calculated from temporal and spatial distribution of conjugate ionospheric disturbances.
3. The ionospheric disturbances present the evidence of the LAIC electric field penetration process.

Abstract

We report observations of ionospheric disturbances in response to North Korea underground nuclear explosion (UNE) on 3 September 2017. By using data from IGS (International GNSS Service) stations and Swarm satellite, geomagnetic conjugate ionospheric disturbances were observed. The observational evidences showed that UNE-generated ionospheric disturbances propagated radially from the UNE epicenter with the velocity of ~ 280 m/s. We propose that the ionospheric disturbances are results of electrodynamic process caused by LAIC (Lithosphere-Atmosphere-Ionosphere Coupling) electric field penetration. LAIC electric field can also be mapped to the conjugate hemispheres along the magnetic field line and consequently cause ionospheric disturbances in conjugate regions. The UNE-generated LAIC electric field penetration plays an important role in the ionospheric disturbances in the region of the nuclear test site nearby and the corresponding geomagnetic conjugate points.

Key words: geomagnetic conjugate ionospheric disturbances; electrodynamic process; LAIC electric field penetration

Ann. Geophys. Discuss., https://doi.org/10.5194/angeo-2018-122
Manuscript under review for journal Ann. Geophys.
Discussion started: 8 November 2018

1 Introduction

Ionospheric disturbances can be generated by various naturally processes such as geomagnetic storms, internal electrodynamic instabilities, coupled upper atmospheric variations and so forth. Furthermore, human activity can also cause evident ionospheric disturbances. Although underground nuclear explosion (UNE) is detonated deep in the lithosphere, ionospheric disturbances related to UNE can also be observed. By using GNSS-TEC observations, *Park et al.* (2011) reported that traveling ionospheric disturbances (TIDs) with phase velocity of ~273 m/s were generated by UNE in the 25 May 2009 North Korea UNE test. They proposed that acoustic gravity waves (AGWs) generated by the UNE can propagate to ionosphere and cause wavelike disturbances.

While the observations of UNE related ionospheric disturbances have been discussed in (*Park et al.*, 2011; 2013), further investigation is still required to understand the mechanism(s) of ionospheric disturbance generation. Lithosphere-atmosphere-ionosphere coupling (LAIC) mechanisms originally proposed to interpret the linkage between ionospheric disturbances and earthquake activities are the most likely explanation for the ionospheric disturbances in response to UNE. The AGWs theory is one part of LAIC mechanisms (*Liu et al.*, 2016; *Maruyama et al.*, 2016). AGWs excited by the unusual events in lithosphere such as an earthquake or an UNE can propagate to ionospheric height and generate TID and electromagnetic disturbances (*Gohberg et al.*, 1990; Mikhailv et al., 2000; *Huang et al.*, 2011; *Ren et al.*, 2012). However, the AGWs mechanism cannot fully explain all the observations related to earthquakes. The electrostatic coupling is another candidate for LAIC mechanisms. During earthquakes,

Ann. Geophys. Discuss., https://doi.org/10.5194/angeo-2018-122
Manuscript under review for journal Ann. Geophys.
Discussion started: 8 November 2018

LAIC electric filed or current can be excited by complex physical and chemical reactions induced by rock rupture and penetrate the ionosphere to promote plasma disturbances by $\boldsymbol{E}\times\boldsymbol{B}$ motion (*Xu et al.*, 2011; *Zhao & Hao*, 2015). *Zhou et al.* (2017) developed an electric field penetration model for LAIC and their simulation results showed that the penetration height of LAIC electric field can reach to 400 km in mid-latitude regions. Because of high electric conductivity of the geomagnetic field lines, LAIC electric field can also be mapped along geomagnetic field lines and cause ionospheric disturbances at the geomagnetic conjugate points (*Ruzhin et al.*, 1998; *Zhang et al., 2009*; *Li & Parrot*, 2017).

In this study, we have used magnetic conjugate GNSS observations and Swarm satellite to investigate the LAIC electric penetration effects of North Korea UNE on 3 September 2017.

2 Instrument and Data

The IGS stations used in this study are located in East Asia and Australia. In order to eliminate the noise and multipath effects of GPS signals, only carrier phase observations are utilized to derive the relative slant total electron content (STEC). The time resolution is about 30 s. The ionospheric pierce points (IPPs) height in this study is assumed at 350 km. The ionospheric disturbances related to UNE are calculated from GNSS observations. In the first step, the numerical third-order horizontal 3-point derivatives of STEC are used for extracting the ionospheric disturbances (*Park et al.*, 2011). Then the wavelet decomposition process is applied to the carrier phase derived

Ann. Geophys. Discuss., https://doi.org/10.5194/angeo-2018-122
Manuscript under review for journal Ann. Geophys.
Discussion started: 8 November 2018

STEC for removing the background noise. The geographical positions of the UNE and the IGS stations are showed in Figure 1.

Swarm mission operated by the European Space Agency (ESA) mainly focuses on the survey of global geomagnetic field and its temporal evolution, which consists of three satellites named Alpha (A), Bravo (B), and Charlie (C). By using the magnetic field data detected by Vector Field Magnetometer (VFM) on Swarm, the ionospheric radial current (IRC) density could be calculated by using spatial gradient of residual magnetic field data through Ampère's law (*Ritter et al.*, 2013). The field-aligned current (FAC) density could be also obtained by the ratio of the IRC density to the sine of the magnetic inclination angle. The FAC density and IRC density used in the study were provided by Swarm level 2 dataset with a time resolution of 1 s. The ionospheric current disturbances associated with UNE can also be calculated by the above method.

3 Observations

According to the measurements of China Earthquake Network Center (CENC), the approximate location of UNE on 3 September, 2017 is at 41.35 °N and 129.11 °E. The explosive time was at 03:30:01 UTC. The geomagnetic *K*p index was less than 3 and AE index was less than 500 nT before and after the UNE, which indicates that the geomagnetic activity was not so active.

Figure 2 shows the time sequences of 3rd-order derivatives of carrier phase derived STEC by GNSS observations from different IGS stations in East Asia and Australia on 3 September 2017. All the GNSS observations from northern and southern hemisphere

Ann. Geophys. Discuss., https://doi.org/10.5194/angeo-2018-122
Manuscript under review for journal Ann. Geophys.
Discussion started: 8 November 2018

showed obvious short-period fluctuations within 2 hours after the UNE. It was also found that time delay after the UNE was different according to different IPPs of GPS signals.

Figure 3 illustrates the satellite Swarm B ionospheric current derivatives. Compared to observed results of ionospheric current in quite time, it was seen that the FAC derivatives and IRC derivatives at conjugate hemispheres both showed obvious short-period fluctuations after the UNE. The ionospheric current disturbances could reach 0.5 $\mu A \cdot m^{-2} \cdot s^{-3}$.

Figure 4 presents the IPPs tracks of STEC derivatives. In order to investigate the propagation velocity of ionospheric disturbances, we assumed that the UNE-generated ionospheric disturbances propagate radially with a certain velocity. Based on the UNE-IPPs horizontal distances and the ionospheric disturbances arrival time, the horizontal propagation velocity of ionospheric disturbances could be estimated by linear fitting model. The horizontal distance from IPPs to epicenter and time delay of the UNE-generated ionospheric disturbances are presented in Figure 5. The value of horizontal velocity obtained by the least square estimation was ~280 m/s.

4 Discussion

By utilizing geomagnetic conjugate GNSS TEC observations and ionospheric current products from Swarm, we introduced the ionospheric disturbances which are considered as a result of the UNE carried out by North Korea on 3 September 2017. The method of the numerical third-order horizontal 3-point derivatives was applied to

Ann. Geophys. Discuss., https://doi.org/10.5194/angeo-2018-122
Manuscript under review for journal Ann. Geophys.
Discussion started: 8 November 2018

the GNSS TEC and the ionospheric current of Swarm to extract the ionospheric disturbances, which can also be found in *Park et al.*, (2011). Ionospheric disturbances derived from GNSS TEC observations in our study are consistent with the results of North Korea UNE on 25 May 2009 obtained by *Park et al.* (2011).

The effects of UNE on the ionosphere could be very similar to that of earthquakes on the ionosphere. In previous studies, AGWs are considered as the most likely mechanism for atmospheric and ionospheric disturbances excited by UNE or earthquakes (*Mikhailov et al.*, 2000; *Che et al.*, 2009; *Garrison et al.*, 2010; *Park et al.*, 2011, 2013; *Park*, 2012; *Yang et al.*, 2012; *Maruyama et al.*, 2016). *Klimenko et al.* (2011) proposed that the ionospheric disturbances were generated by small-scale internal gravity waves (IGWs) through propagation and dissipation processes during seismic activity. However, AGWs mechanism cannot explain the geomagnetic conjugate observations in Figure 2, because mechanical waves such as AGWs cannot propagate to the other hemisphere.

Recent researches have shown that earthquake ionospheric disturbances could be attributed to not only the AGW mechanism but also the electrostatic coupling, which means the electric field or current penetration into ionosphere induced by earthquakes. Based on the observations of INTERCOSMOS-BULGARIA-1300 satellite and DEMETER satellite, *Gousheva et al.* (2008, 2009) and *Zhang et al.* (2014) reported ionospheric quasi-static electric field perturbations during seismic activities. *Pulinets et al.* (2000) proposed a quasi-electrostatic model for the LAIC mechanism. The simulation results indicated the abnormal electric field induced by an earthquake can

Ann. Geophys. Discuss., https://doi.org/10.5194/angeo-2018-122
Manuscript under review for journal Ann. Geophys.
Discussion started: 8 November 2018

penetrate into the ionosphere to cause the ionospheric electric field disturbances. The enhancement of TEC at the epicenter and its geomagnetic conjugate points were reported by *Liu et al.* (2011), which indicated that the earthquake-generated electric field penetration can be mapped along geomagnetic field lines to promote ionospheric disturbances at its conjugate points by electrodynamic process through $\boldsymbol{E}\times\boldsymbol{B}$ drift. Therefore, the geomagnetic conjugation effects of ionospheric disturbances in Figure 2 can be explained by the UNE-generated electric field penetration. A schematic sketch of geomagnetic conjugate effect related to UNE in the region of the nuclear test site nearby and the corresponding geomagnetic conjugate region is shown in Figure 6. The UNE-generated electric field or current penetrates into the ionosphere and further generates an abnormal electric field at ionospheric altitude. The distribution of ionospheric electric filed showed in Figure 6 were calculated by LAIC electric field penetration model proposed by *Zhou et al.* (2017). Because of the existence of high conductivity of geomagnetic field, the abnormal ionospheric electric filed could be mapped along geomagnetic field lines. Geomagnetic conjugate ionospheric disturbances could be generated by abnormal ionospheric electric filed through $\boldsymbol{E}\times\boldsymbol{B}$ drift. Our study provides observational evidences of LAIC electric penetration other than acoustic gravity wave mechanism.

Geomagnetic conjugate observations in ionosphere have been reported by a few researchers. *Otsuka et al.* (2002; 2004) reported simultaneous observations of equatorial airglow depletions and medium-scale TIDs at geomagnetic conjugate points in both hemispheres by two all-sky imagers. Their results also suggested that polarization electric field, which is important for airglow depletion and MSTIDs generation, can be mapped along the field lines.

In our observations, we found that the ionospheric disturbances in both hemispheres caused by the UNE-generated electric field penetration propagated radially at the velocity of roughly 280 m/s in Figure 4 and Figure 5. LAIC electric field can be roughly estimated to be 11 mV/m, which is consistent with the magnitude of the earthquake-generated ionospheric electric field presented by *Zhang et al.* (2014). Figure 3 presents the results of the ionospheric current disturbances detected by the satellite Swarm B after the UNE. The reason may be that the ionospheric disturbances from the UNE propagate here to generate the current disturbances by electrodynamic process.

5 Summary

In this study, we have shown that the geomagnetic conjugate observations of GNSS TEC and ionospheric current from Swarm considered as a response to North Korea UNE on 3 September 2017. The LAIC electric penetration effects of UNE have been discussed in details. The main results are summarized as follows:

1. The ionospheric TEC and current disturbances were observed in both hemispheres after the UNE. According to the spatial-temporal relation, UNE-generated ionospheric disturbances propagated radially from the explosion epicenter with the velocity of ~ 280 m/s.

2. The ionospheric disturbances may be caused by LAIC electric penetration rather than AGWs. LAIC electric field induced by UNE penetrates into the ionosphere and causes

plasma density disturbances near the nuclear test cite and its conjugate points by electrodynamic process.

Acknowledgments

We thank the use of GPS-TEC data from IGS Data Center of Wuhan University (http://www.igs.gnsswhu.cn/index.php/Home/DataProduct/igs.html). We also acknowledge the ESA for the Swarm data (https://earth.esa.int/web/guest/swarm/data-access). The work is supported by the National Natural Science Foundation of China (NSFC grant No. 41574146 and 41774162).

Ann. Geophys. Discuss., https://doi.org/10.5194/angeo-2018-122
Manuscript under review for journal Ann. Geophys.
Discussion started: 8 November 2018

Annales Geophysicae Discussions
Open Access

References

Che, I.-Y., Kim, T. S., Jeon, J.-S., and Lee, H.-I.: Infrasound observation of the apparent North Korean nuclear test of 25 May 2009, Geophys. Res. Lett., 36, L22802, 2009.

Garrison, J. L., Yang, Y.-M., and Lee, S.-C.: Observations of ionospheric disturbances coincident with North Korean underground nuclear tests, Abstract SA43B-1754 presented at 2010 Fall Meeting, AGU, San Francisco, Calif., 13–17 Dec, 2010.

Gohberg, M. B., Pilipenlco, V. A., Pokhotelov, O. A., and Partasaraty, S.: Acoustic influence of underground nuclear explosion as source of electrostatic turbulence in magnetosphere, Doklady AN SSSR, 313(N3), P568, 1990.

Gousheva, M., Danov, D., Hristov, P., and Matova, M.: Quasi-static electric fields phenomena in the ionosphere associated with pre- and post-earthquake effects, Nat. Hazards Earth Syst. Sci., 8, 101-107, 2008.

Gousheva, M., Danov, D., Hristov, P., and Matova, M.: Ionospheric quasi-static electric field anomalies during seismic activity in August–September 1981, Nat. Hazards Earth Syst. Sci., 9, 3-15, 2009.

Huang, Q.: Retrospective investigation of geophysical data possibly associated with the Ms8.0 Wenchuan earthquake in Sichuan, China, J. Asian Earth Sci., 41(4-5): 421-427, 2011.

Klimenko, M. V., Klimenko, V. V., Karpov, I. V., and Zakharenkova, I. E.: Simulation of Seismo-Ionospheric Effects Initiated by Internal Gravity Waves, Russ. J. Phys. Chem. B, 5(3), 393-401, 2011.

Li, M., and Parrot, M.: Statistical analysis of the ionospheric ion density recorded by

DEMETER in the epicenter areas of earthquakes as well as in their magnetically conjugate point area, Adv. Space Res., 61(3), 974-984, 2017.

Liu, J. Y., Le, H., Chen, Y. I., Chen, C. H., Liu, L., Wan, W., Su, Y. Z., Sun, Y. Y., Lin, C. H., and Chen, M. Q.: Observations and simulations of seismo-ionospheric GPS total electron content anomalies before the 12 January 2010 M7 Haiti earthquake, J. Geophys. Res., 116, A04302, 2011.

Liu, J. Y., Chen, C. H., Sun, Y. Y., Chen, C. H., Tsai, H. F., Yen, H. Y., Chum, J., Lastovicka, J., Yang, Q. S., Chen, W. S., and Wen, S.: The vertical propagation of disturbances triggered by seismic waves of the 11 March 2011 M9.0 Tohoku earthquake over Taiwan, Geophys. Res. Lett., 43(4), 1759-1765, 2016.

Maruyama, T., Yusupov, K., and Akchurin, A.: Ionosonde tracking of infrasound wavefronts in the thermosphere launched by seismic waves after the 2010 M8.8 Chile earthquake, J. Geophys. Res. Space Physics., 121, 2683-2692, 2016.

Mikhailov, Y. M., Mikhailova, G. A., and Kapustina, O. V.: VLF effects in the outer ionosphere from the underground nuclear explosion on Novaya Zemlya island on 24 October, 1990 (INTERCOSMOS 24 satellite data), Phys. Chem. Earth Part C, 25(1–2), 93–96, 2000.

Otsuka, Y., Shiokawa, K., Ogawa, T., and Wilkinson, P.: Geomagnetic conjugate observations of equatorial airglow depletions, Geophys. Res. Lett., *29*, 1753, 2002.

Otsuka, Y., Shiokawa, K., Ogawa, T., and Wilkinson, P.: Geomagnetic conjugate observations of medium-scale traveling ionospheric disturbances at midlatitude using all-sky airglow imagers, Geophys. Res. Lett., 31, L15803, 2004.

Ann. Geophys. Discuss., https://doi.org/10.5194/angeo-2018-122
Manuscript under review for journal Ann. Geophys.
Discussion started: 8 November 2018

Park, J., Frese, R. R. B. von, Grejner-Brzezinska, D. A., Morton, Y., and Gaya-Pique, L. R.: Ionospheric detection of the 25 May 2009 North Korean underground nuclear test, Geophys. Res. Lett., 38, L22802, 2011.

Park, J.: Ionospheric monitoring by the global navigation satellite system (GNSS), PhD dissertation, The Ohio State University, Columbus, OH, USA, 2012.

Park, J., Helmboldt, J., Grejner-Brzezinska, D. A., Frese, R. R. B. von, and Wilson, T. L.: Ionospheric observations of underground nuclear explosions (UNE) using GPS and the Very Large Array, Radio Sci., 48, 463–469, 2013.

Pulinets, S. A., Boyarchuk, K. A., Hegai, V. V., Kim, V. P., and Lomonosov, A. M.: Quasi-electrostatic model of atmosphere-thermosphere-ionosphere coupling, Adv. Space Res., 26(8), 1209-1218, 2000.

Ren, H., Chen, X., and Huang, Q.: Numerical simulation of co-seismic electromagnetic fields associated with seismic waves due to finite faulting in porous media, Geophys. J. Int., 188, 925-944, 2012.

Ritter, P., Lühr, H., and Rauberg, J.: Determining field-aligned currents with the Swarm constellation mission, Earth Planets Space, 65, 1285-1294, 2013.

Ruzhin, Y. Y., Larkina, V. I., and Depueva, A. K.: Earthquake precursors in magnetically conjugated ionosphere regions, Adv. Space Res., 21(3), 525-528, 1998.

Xu, T., Hu, Y., Wu, J., Wu, Z., Li, C., Xu, Z., and Suo, Y.: Anomalous enhancement of electric field derived from ionosonde data before the great Wenchuan earthquake, Adv. Space Res., 47(6), 1001-1005, 2011.

Yang, Y.-M., Garrison, J. L., and Lee, S. C.: Ionospheric disturbances observed coincident with the 2006 and 2009 North Korean underground nuclear tests, Geophys. Res. Lett., 39, L02103, 2012.

Zhao, B., and Hao, Y.: Ionospheric and geomagnetic disturbances caused by the 2008 Wenchuan earthquake: A revisit, J. Geophys. Res. Space Phys., 120, 5758–5777, 2015.

Zhang, X., Shen, X., Liu, J., Ouyang, X., Qian, J., and Zhao, S.: Analysis of ionospheric plasma perturbations before Wenchuan earthquake, Nat. Hazards Earth Syst. Sci., 9, 1259-1266, 2009.

Zhang, X., Shen, X., Zhao, S., Yao, L., Ouyang, X., and Qian, J.: The characteristics of quasistatic electric field perturbations observed by DEMETER satellite before large earthquakes, J. Asian Earth Sci., 79(2), 42-52, 2014.

Zhou, C., Liu, Y., Zhao, S., Liu, J., Zhang, X., Huang, J., Shen, X., Ni, B., and Zhao, Z.: An electric field penetration model for seismo-ionospheric research, Adv. Space Res., 60(10), 2217-2232, 2017.

Ann. Geophys. Discuss., https://doi.org/10.5194/angeo-2018-122
Manuscript under review for journal Ann. Geophys.
Discussion started: 8 November 2018

Figure Captions

Figure 1. The positions of UNE and IGS stations. The position of 3 September 2017 North Korea UNE is represented by black hollow start mark. The locations of IGS stations in both hemispheres are represented by red and blue squares, respectively.

Figure 2. The time sequences of 3-order derivatives of carrier phase derived STEC by GNSS observations from different IGS stations in East Asia (left and middle column) and Australia (right column) on 3 September 2017. The blue lines indicate the wavelet de-noised 3-order derivative of STEC. The black lines indicate the GPS signal's elevation between the GNSS satellite and IGS stations. The explosive time is represented by the red line.

Figure 3. Results of Swarm B ionospheric current data analysis for the 2017 UNE: (a), (b) the FAC, (c), (d) the IRC. Left and right sides indicate observations of Swarm B on 2 September 2017 (quite time) and 3 September 2017 (UNE time), respectively. The ionospheric current disturbances in response to UNE are represented by the red rectangles.

Figure 4. The IPPs tracks of STEC derivatives. The red lines indicate the IPPs tracks obtained by IGS stations in the northern hemisphere. The blue lines indicate the magnetic conjugate positions of the IPPs tracks obtained by IGS stations in the southern hemisphere. The positions of the maximum amplitudes of STEC derivatives in the northern hemisphere are represented by red triangles. The geomagnetic conjugate positions of the maximum amplitudes of STEC derivatives in the southern hemisphere are represented by blue triangles.

Figure 5. Horizontal distance-time data for the UNE-generated ionospheric disturbances. The black line indicates the fitting curve obtained by the least square method. The gray lines represent the boundaries of 95% confidence intervals. The red and blue triangles indicate same meanings as in Figure 4. The black triangle represents the position of ionospheric current disturbances in the northern hemisphere. The green triangle represents the geomagnetic conjugate position of ionospheric current disturbances in the southern hemisphere.

Ann. Geophys. Discuss., https://doi.org/10.5194/angeo-2018-122
Manuscript under review for journal Ann. Geophys.
Discussion started: 8 November 2018

Figure 6. A sketch of geomagnetic conjugate effect related to UNE in the region of the nuclear test site nearby and the corresponding geomagnetic conjugate region.

Ann. Geophys. Discuss., https://doi.org/10.5194/angeo-2018-122
Manuscript under review for journal Ann. Geophys.
Discussion started: 8 November 2018

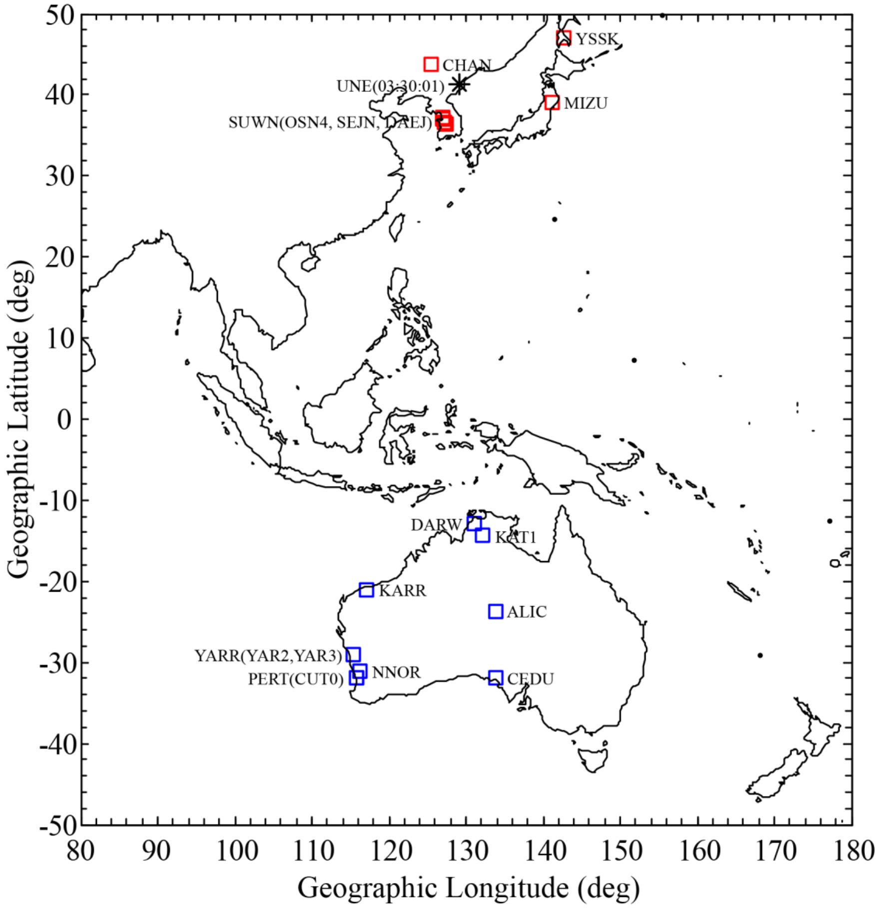

Figure 1. The positions of UNE and IGS stations. The position of 3 September 2017 North Korea UNE is represented by black hollow start mark. The locations of IGS stations in both hemisphere are represented by red and blue squares, respectively.

Ann. Geophys. Discuss., https://doi.org/10.5194/angeo-2018-122
Manuscript under review for journal Ann. Geophys.
Discussion started: 8 November 2018

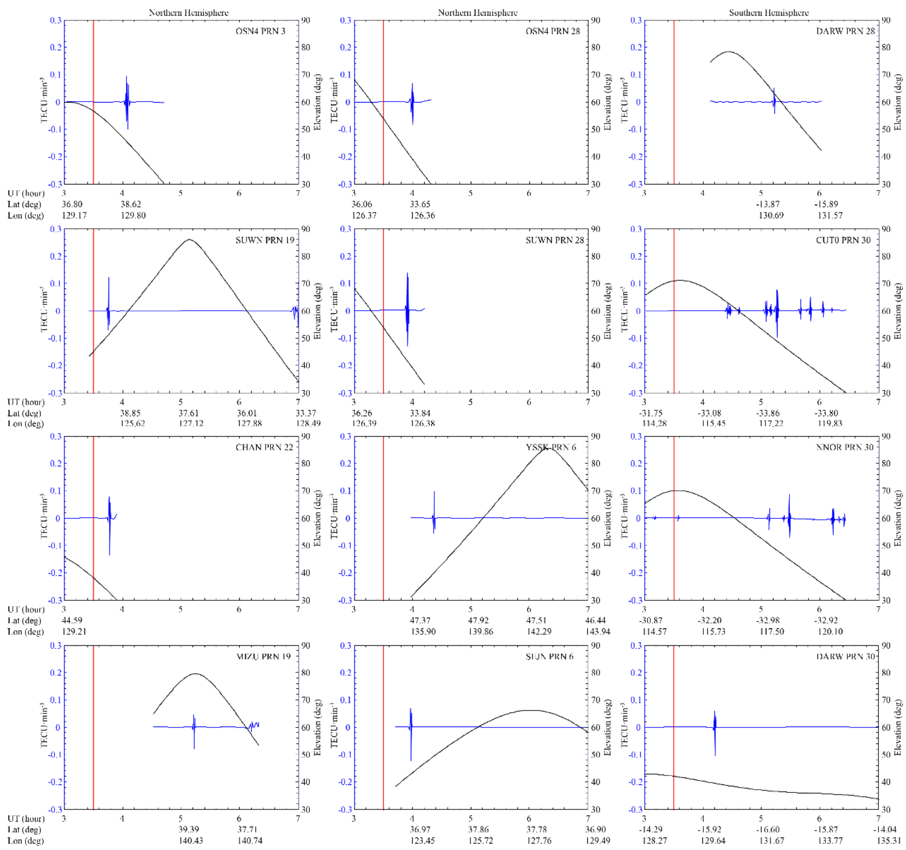

Figure 2. The time sequences of 3-order derivatives of carrier phase derived STEC by GNSS observations from different IGS stations in East Asia (left and middle column) and Australia (right column) on 3 September 2017. The blue lines indicate the wavelet de-noised 3-order derivative of STEC. The black lines indicate the GPS signal's elevation angle between the GNSS satellite and IGS stations. The explosive time is represented by the red line.

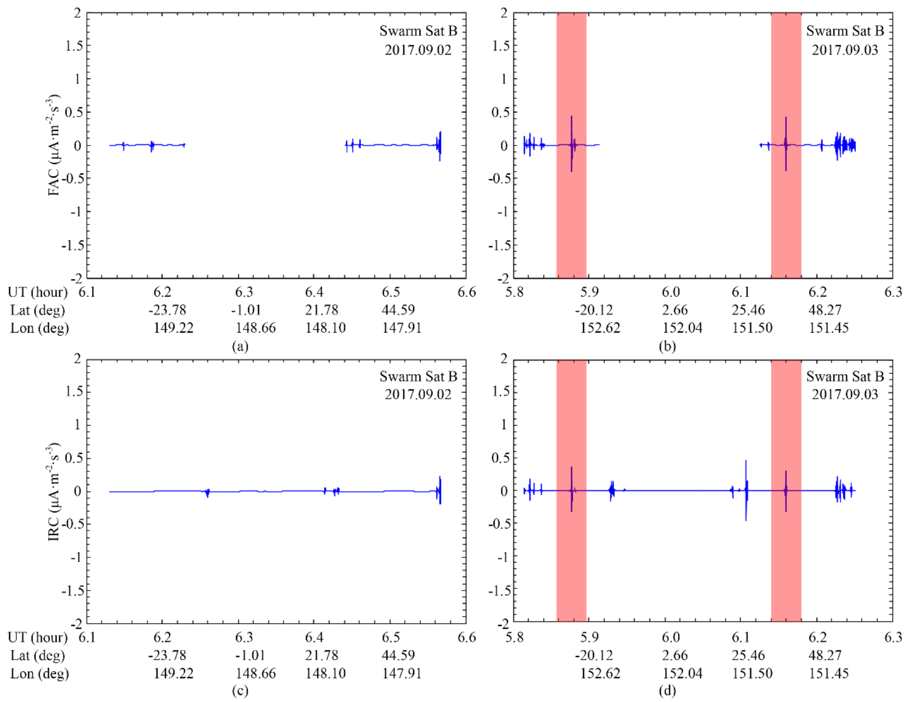

Figure 3. Results of Swarm B ionospheric current data analysis for the 2017 UNE: (a), (b) the FAC, (c), (d) the IRC. Left and right sides indicate observations of Swarm B on 2 September 2017 (quite time) and 3 September 2017 (UNE time), respectively. The ionospheric current disturbances in response to UNE are represented by the red rectangles.

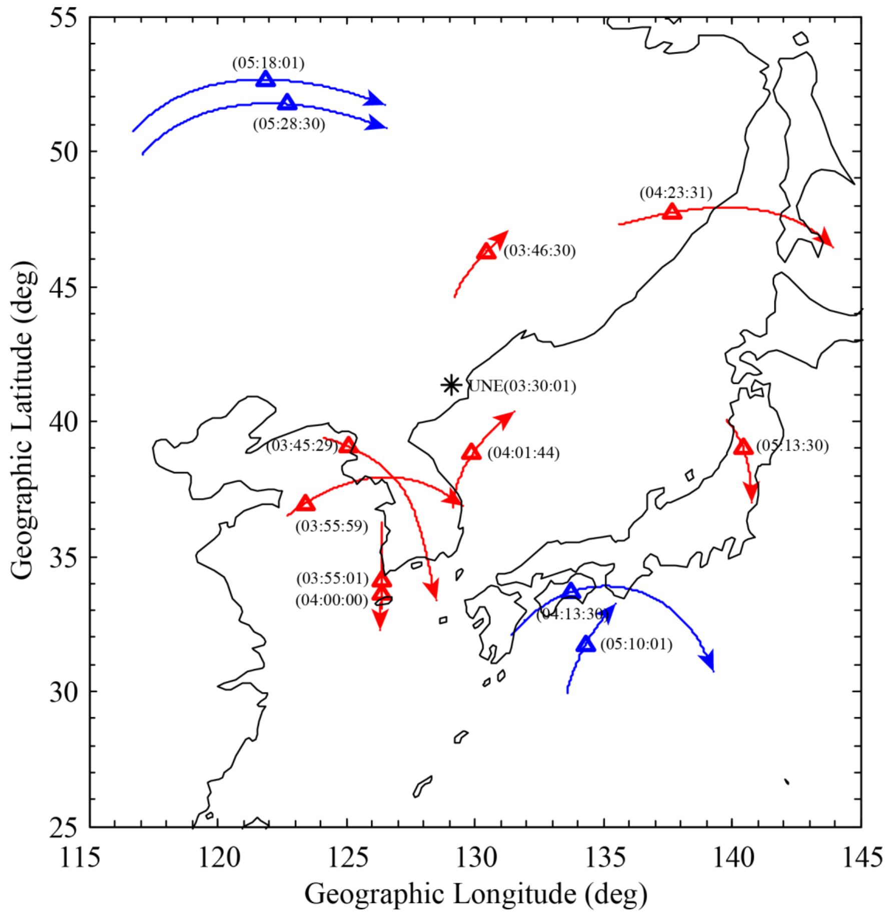

Figure 4. The IPPs tracks of STEC derivatives. The red lines indicate the IPPs tracks obtained by IGS stations in the northern hemisphere. The blue lines indicate the magnetic conjugate positions of the IPPs tracks obtained by IGS stations in the southern hemisphere. The positions of the maximum amplitudes of STEC derivatives in the northern hemisphere are represented by red triangles. The geomagnetic conjugate positions of the maximum amplitudes of STEC derivatives in the southern hemisphere are represented by blue triangles.

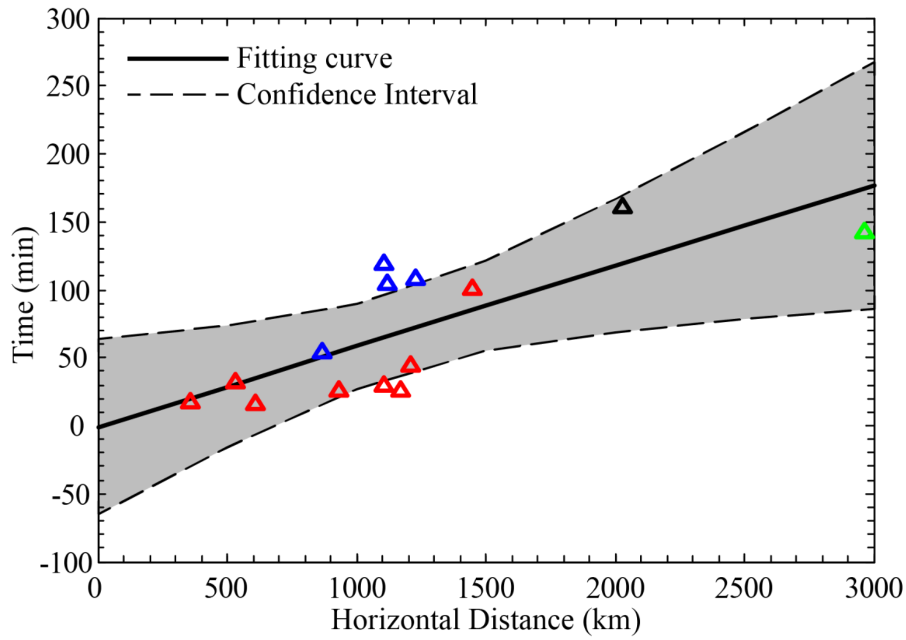

Figure 5. Horizontal distance-time data for the UNE-generated ionospheric disturbances. The black line indicates the fitting curve obtained by the least square method. The gray lines represent the boundaries of 95% confidence intervals. The red and blue triangles indicate same meanings as in Figure 4. The black triangle represents the position of ionospheric current disturbances in the northern hemisphere. The green triangle represents the geomagnetic conjugate position of ionospheric current disturbances in the southern hemisphere.

Ann. Geophys. Discuss., https://doi.org/10.5194/angeo-2018-122
Manuscript under review for journal Ann. Geophys.
Discussion started: 8 November 2018

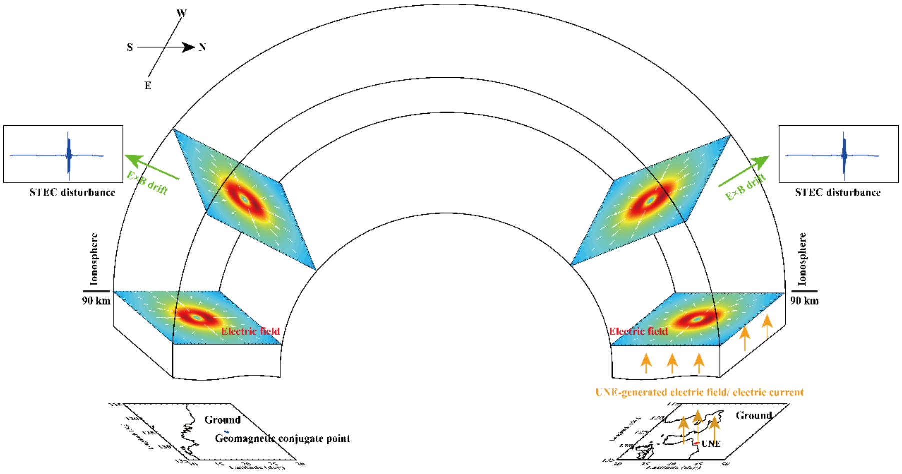

Figure 6. A sketch of geomagnetic conjugate effect related to UNE in the region of the nuclear test site nearby and the corresponding geomagnetic conjugate region.